Space moving target detection and tracking method in complex background

Ping-Yue Lv, Sheng-Li Sun, Chang-Qing Lin, Gao-Rui Liu

PII: S1350-4495(17)30600-X
DOI: https://doi.org/10.1016/j.infrared.2018.03.007
Reference: INFPHY 2510

To appear in: *Infrared Physics & Technology*

Received Date: 24 September 2017
Revised Date: 5 March 2018
Accepted Date: 5 March 2018

Please cite this article as: P-Y. Lv, S-L. Sun, C-Q. Lin, G-R. Liu, Space moving target detection and tracking method in complex background, *Infrared Physics & Technology* (2018), doi: https://doi.org/10.1016/j.infrared.2018.03.007

Summary of changes

Ping-Yue Lv [abc], Sheng-Li Sun[ab], Chang-Qing Lin [ab], Gao-Rui Liu [abc]
(a CAS Key Laboratory of Infrared System Detection and Imaging Technology, Shanghai Institute of Technical Physics, Shanghai 200083; b Shanghai Institute of Technical Physics of the Chinese Academy of Sciences, Shanghai 200083; c University of Chinese Academy of Sciences, Beijing 100049)

Abstract

First, we would like to sincerely thank the editors and the reviewers for their valuable comments, suggestions and encouragement on our revised paper (INFPHY_2017_516_R1). Listed below are the revision comments about Highlights according to reviewer 2.

Comments by Reviewer 2:

(1) For the 2nd point, please delete 'and better result';

(2) For the 3rd point, I suggest the authors use the following expression: 'Our method outperforms other state-of-the-art algorithms in both image sequences with real targets and simulated targets';

(3) For the 4th point, a simpler expression as 'The algorithm proposed can solve the space-based weak moving target detection problem when SRC≈1 or even SCR<1'may be better.

The following is a modified version of highlights:

Highlights

1. A target enhancing algorithm based on gray scale difference (GSD) is proposed, which can obtains high SCR gain (⩾50).
2. A complete point target detection and processing model is proposed. Experiment results show that the model is obviously better than other state-of-art algorithms in terms of SCR gain and background suppression factor (BSF).
3. Our method outperforms other state-of-the-art algorithms in both image sequences with real targets and simulated targets.
4. The algorithm proposed can solve the space-based weak moving target detection problem when SCR≈1 or even SCR<1.

Space moving target detection and tracking method in complex background

Ping-Yue Lv [abc], Sheng-Li Sun[ab], Chang-Qing Lin [ab], Gao-Rui Liu [abc]
(a CAS Key Laboratory of Infrared System Detection and Imaging Technology, Shanghai Institute of Technical Physics, Shanghai 200083; b Shanghai Institute of Technical Physics of the Chinese Academy of Sciences, Shanghai 200083; c University of Chinese Academy of Sciences, Beijing 100049)

ABSTRACT

The background of the space-borne detectors in real space-based environment is extremely complex and the signal-to-clutter ratio is very low (SCR≈1), which increases the difficulty for detecting space moving targets. In order to solve this problem, an algorithm combining background suppression processing based on two-dimensional least mean square filter (TDLMS) and target enhancement based on neighborhood gray-scale difference (GSD) is proposed in this paper. The latter can filter out most of the residual background clutter processed by the former such as cloud edge. Through this procedure, both global and local SCR have obtained substantial improvement, indicating that the target has been greatly enhanced. After removing the detector's inherent clutter region through connected domain processing, the image only contains the target point and the isolated noise, in which the isolated noise could be filtered out effectively through multi-frame association. The proposed algorithm in this paper has been compared with some state-of-the-art algorithms for moving target detection and tracking tasks. The experimental results show that the performance of this algorithm is the best in terms of SCR gain, background suppression factor (BSF) and detection results.

Keywords: Weak point target, low SCR, complex background, GSD, TDLMS.

1. INTRODUCTION

Study of space-borne weak target detection in complex background has been one of the hot issues in space field research. The distant imaging distance makes the target appear in the image plane as a weak point, which occupies only one or several pixels, no contours, textures or shape characteristics. Meanwhile, due to cloud clutter and other background clutter, the target is often submerged in the background, coupled with the inherent noise of the system noise, weak target detection is of great difficulty. Space target detection mainly relies on target's gray features and motion characteristics. The former uses the difference between the intensity of the target and the neighborhood to suppress most of the background and clutter, and the latter uses the regularity of target motion to remove most of the isolated noise.

Related research focuses on single-frame suppression[12] and multi-frame correlation detection[3]. In the case of weak point target detection, it is necessary to carry out background suppression and target enhancement, which directly affect the accuracy of detection. The two-dimensional least square algorithm[4] proposed by Mohiy M.Hadhoud and David W.Thomas is an adaptive filter algorithm that increases the signal-to-noise ratio by enhancing the target and background contrast. By setting a sliding window, the filter iteratively updates weight matrixes while scanning an image, when it scans the target area, the weight matrix is the continuation of the previous iteration because of the weak correlation of target pixels and background pixels, , and therefore the filter ignores the target. Morphology top-hat filter[56], as a classic non-linear filter, can effectively enhance the

point target. Its fast running speed makes it easily expand to real-time systems, however, it is more suitable for smooth background images. The max-mean and max-median algorithms[7] proposed by Deshpande S.D. et al. are two effective target enhancement algorithms，the former calculates the average values of the horizontal diagonal, the vertical diagonal, the left diagonal, and the right diagonal of the neighborhood pixels respectively, and then takes the maximum value as the estimate value of the central pixel; the latter is to take the median of the four directions and then the maximum is taken as the estimate value. The experimental results show that the residual images after either of the two background estimations can enhance the target. NL-means (non-local means) algorithm[8910] proposed by Buades.A et al., performs well in image de-noising. Theoretically, its essence is to replace each pixel by an average weighted estimate of all other pixels in the image. The contribution of each pixel to the current scanning pixel is based on the degree of similarity of the neighborhood. The essence of this algorithm, when applied to the field of weak target detection[11], is to regard the small target as a noise point, and then to detect the target in the residual image of the original image and the background estimate image. The local inverse entropy[12] proposed by He D, Wei Y.T et al. combines the idea of local entropy and inverse entropy[13]. Its principle is that the weak target point may have a great influence on the gray values of the neighborhood. It essentially is a background suppression operator. The nucleus similarity density method[14] proposed by Zhao F et al. combines spatial and grayscale properties to generate a nucleus estimate for each pixel, which can be a value basis for linear filtering and non-linear filtering.

Tested in real space-based image sequences, the two-dimensional least mean square (TDLMS) algorithm is superior to other algorithms for single frame background suppression and point target enhancement, the shortcoming is that there are still residual background clutters. There are many improvements based on this algorithm. Cao et al. proposed am improved TDLMS algorithm[15] based on neighborhood analysis. The main improvement is to set an adaptive iterative step size adjustment and take more neighborhood information into consideration, extending one sliding window to five windows and using some fusion strategies to predict the weighted values of the central pixel. Bae Tae-Wuk et al. proposed an edge-directional TDLMS method[16] for infrared small target detection, which is a further improvement of the algorithm proposed by Cao et al. Edge directional TDLMS extends five windows to nine windows, each generating a predictive value based on horizontal, vertical, left diagonal, right diagonal pixels. The similarity degree of the values determines the value of the central pixel prediction and updates the weight matrix accordingly. It is designed to filter out smooth cloud edge clutter. On the basis of TDLMS, Wan L.L et al. proposed a filter[17] based on TDLMS with neighborhood information, which still sets nine neighborhood windows, except that it uses neighborhood information instead of edge-based information. It takes into account the relationship between the other eight prediction windows and the central window as a basis for weight matrix update and predictive value output. As for these improved algorithms for TDLMS, they are more suitable for the situation where background is not very complicated and concludes smooth cloud edge. For real applications, ups and downs of background are very serious and it is difficult to have smooth edge characteristics, especially for cloud and land backgrounds. Therefore, applying these algorithms to the real world does have restrictions to a certain degree. It is not enough to simply improve one certain background suppression algorithm, and it is necessary to re-enhance the target after suppression.

This paper assumes that the non-uniformity correction has been finished and the system background noise has been eliminated, only image sequences downloaded from satellite to foundation are processed. As for space moving target detection and tracking, the first step is to suppress background clutter. Background contains a large number of cloud clutter and noise, which is the main factor leading to high false alarm rate. Therefore, combined with actual application, this paper first implements background suppression and target enhancement to improve the signal-to-clutter ratio. TDLMS performs well in real space-based image sequences for

single-frame background suppression and target enhancement, but can only remove some of the internal background clutter, the residual clutter is even more difficult to remove, which contains the edge of the cloud, the system inherent noise and other gray-scale ups and downs. In this paper, a threshold segmentation algorithm combining neighborhood gray-scale difference metric and morphological operator is proposed to filter out the residual background clutter interference. After this processing, there are still some patchy noise areas in the image due to the inherent noise of the detector. Since the real target size is small (no more than 3×3 pixel size), these noise regions are removed by connected domain segmentation operation. Finally, according to the regularity of the real target movement, the target trajectory in the image sequence is extracted by multi-frame association. The experimental results show that the proposed processing model can effectively detect both simulated and real targets.

The structure of this paper is as follows: Section 1 introduces the research background of this paper; Section 2 describes the preprocessing algorithm: two-dimensional least mean square filter (TDLMS), and the selection of step size, an important parameter of TDLMS, is explained ; Section 3 elaborates the proposed neighborhood gray-scale difference metric re-enhancement algorithm; in Section 4, the whole process of target extraction is expounded, and the performance of the algorithm model proposed in this paper is explained; the experimental results and related explanation are carried out in Section 5; Section 6 provides the conclusion and future work.

2. PREPROCESSING

2.1 Two-dimensional least mean square (TDLMS)

TDLMS algorithm is first proposed by Mohiy.M.Hadhoud and David.W. Thomas in 1988. It is derived from the least mean square error (LMS) filter (that is, the Wiener filter), based on the random variables of image and noise, an attempt is made to find an estimate of the undisturbed image so that the mean square error of the noise image and the restored image is minimized. For an input image X of size$M \times N$, a filter window of $R \times R$ is set, scanning from left to right, from top to bottom for each pixel, as for a certain pixel(x, y), its estimated value $E(x, y)$ is expressed as follows:

$$\mathrm{E(x,y)} = \sum_{i=0}^{R-1} \sum_{j=0}^{R-1} W_k(i,j) X(x-i, y-j) \quad (1)$$

In the above formula, $x = (0,1,2,\dots,M-1), y = (0,1,2,\dots,N-1)$. The filter iteratively updates the weight matrixW_k. This paper uses sliding windows for scanning operations from top to bottom and from left to right, therefore, $k = x * N + y$. The weight matrix is updated using the steepest descent method, the formula is:

$$W_{k+1}(i,j) = W_k(i,j) + \mu e_k X(x-i, y-j) \quad (2)$$

Where, e_k is an estimated error value, that is, the difference between the estimated value of the output and the expected value. In this paper, $e_k = X(x,y) - E(x,y)$. The initialized weight matrix W_0 is the Gaussian filter matrix. μ is the iterative step size, the selection of μ is discussed in detail in Section 2.2.

2.2 Selection of step size

For TDLMS, the step size μ is an important parameter that affects the weight update and the prediction result. Since the residual image is the background-suppressed image, TDLMS algorithm needs to ignore the target area and preserve the background edge as much as possible. The step size, μ, as a parameter that regulates the convergence speed of the filter, as mentioned in reference [15], should ideally decreases as the filter processes the target pixel and increases at the background edge. However, the authors have found that through experimentation, adaptive step size does not seem to significantly increase the intensity of the target or increase the probability of detection for the low SCR environment (SCR≈1) mentioned in this article. At the same time,

adaptive step size adjustment inevitably introduces more algorithmic overhead. In order to seek a reasonable step size value, combined with the scope of this article, the following step size selection strategy is discussed.

a) Enhancement for target and background pixels. As mentioned above, a reasonable step size should be able to ignore the target pixels and keep the background pixels. When the step size is too small, more false alarms are introduced; if the step size is too large, it may cause targets missing. Therefore, by experimenting and experiences, we define a range $[10^{-7},\ 10^{-5}]$ as the value range of step size. (In fact, when μ is less than10^{-7}, to some extent, TDLMS can also effectively enhance the target, but introduces more false alarms, therefore it is not considered here). For infrared images of three different backgrounds (the average signal-to-noise ratio is about 1), take one target center pixel, two cloud edge pixels and two flat background pixels respectively. The result of enhancement through TDLMS is shown in Fig.1. Fig.1 shows the trend of the intensity of the target pixel and the four non-target pixels changing with step size.

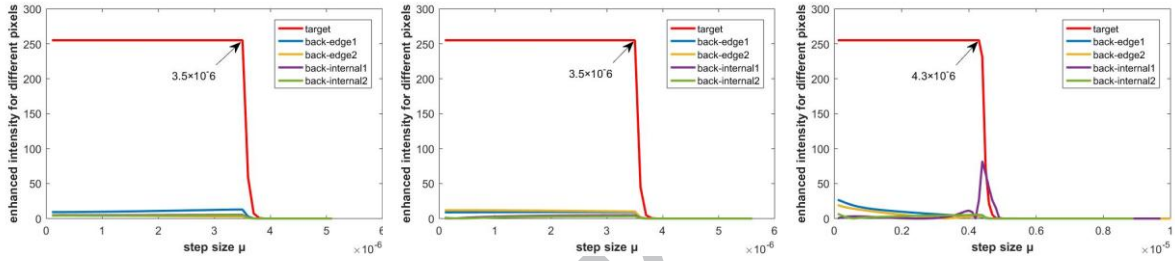

Fig. 1 Enhancement for target pixels, cloud edge pixels, smooth background pixels using variable step sizes. Three images represent three different backgrounds.

From Fig.1, for the three sequences with average signal-to-noise ratios of about 1, respectively, quantized bits of 8 bits, in the range of $[10^{-7},\ 3.5\times10^{-6}]$, the filter is in a steady state, and the "target" representing the trend of the target center pixel shows that the target region can be almost completely neglected, while the other curves characterizing non-target pixels show that most of the edge pixels and smooth background pixels can be estimated as background pixels in the preprocessing stage and get better suppression in the residual image (target enhancement image). For values greater than the step size indicated by the arrow, the filter comes to an unstable state and the target enhancement effect is drastically reduced.

b) The effect on accuracy of background estimation. As a background estimation algorithm in the preprocessing stage, TDLMS needs to ensure as much as possible that the background is effectively estimated when the filter is in a stable range, so as to filter out most of the background. In order to measure the degree of similarity of the background estimation, the concept of "mean absolute error (MAE)" is introduced here. Likewise, for an M × N image X, the calculation formula of MAE is as follows:

$$\mathrm{MAE} = \frac{1}{M\times N}\sum_{i=1}^{M}\sum_{j=1}^{N} abs[X(i,j) - E(i,j)] \quad (3)$$

In the above equation, E represents the background estimation image. $abs[X(i,j) - E(i,j)]$ represents the absolute value of the difference between the original value and the estimated value of the pixel (i,j). Randomly selecting one image of each sequence mentioned in a) (average signal-to-noise ratio is about 1), using the range of $[10^{-7},\ 10^{-5}]$, Fig.2 shows the relationship between average absolute error and step size. The position marked by the arrow is the step size at which the MAE starts to increase significantly (the filter starts to enter an unstable state), after which the MAE values enter the oscillating state (Obviously, these values are consistent with the step sizes at the time when the target enhancement performance decreases in a)). The steady-state step size value before the filter enters the oscillating state can enhance the target effectively, which also verifies the

conclusion obtained in a). The ellipse in Fig.2 points out the very step size that makes MAE infinite, which are respectively 5×10^{-6}, 4.9×10^{-6}, 7.7×10^{-6}. The step size values greater than these values are completely invalid.

c) Variable SCR. Using the same step size interval as in a) and b), Fig.3 shows the intensities of the target enhancement for several SCR environments. The arrow in the Fig.3 shows the step size value when the filter is out of steady state and the performance begins to decay (in accordance with the order of SCR from low to high, 4.3×10^{-6}, 4.3×10^{-6}, 2.9×10^{-6}, 1.7×10^{-6},respectively). In combination with Fig.1, for non-target pixels the conclusion also holds, and the higher the signal-to-clutter ratio, the smaller the step size value. At the same time, when SCR≥1, there is a stable range of fixed step values, in this range, the pretreatment stage TDLMS can maximize the target. For a background of SCR = 0.68 (without loss of generality, it can be extrapolated to a very low SCR environment), it can be seen from the figure that the maximum of the target can only be increased to half of that of the other cases. This kind of decline is caused by the low intensity of the target itself.

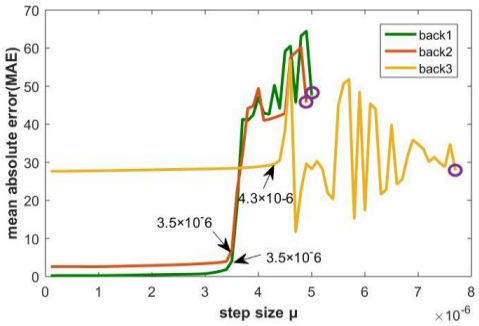

Fig. 2 Relationship between step size and MAE

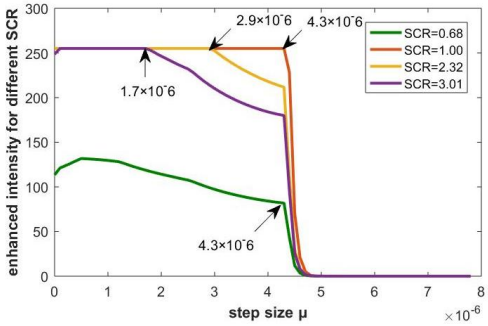

Fig. 3 The influence of step size on target enhancement under different SCR environment

It is worth mentioning that, although the above analysis is based on a specific experimental sequences, but they are not without loss of generality. It is can be concluded that, in the case of SCR≤3, the step size value $10^{-6}$of the filter can represent a stable filter state. Based on the above analysis, a) and b) respectively discuss the relationship between step size and target intensity, step size and MAE when SCR≈1, and give the range of effective step size. Furthermore, the effect of step size on the performance of enhancement under different SCR is discussed in c). The conclusion can provide reference for this paper and theoretical basis for further research. Combined with the above analysis results, since fixed step size can obtain effective enhancing results in pretreatment stage, provide a stable state for the filter and the computational overhead is small, therefore here we select the step size 10^{-6} as the fixed step size.

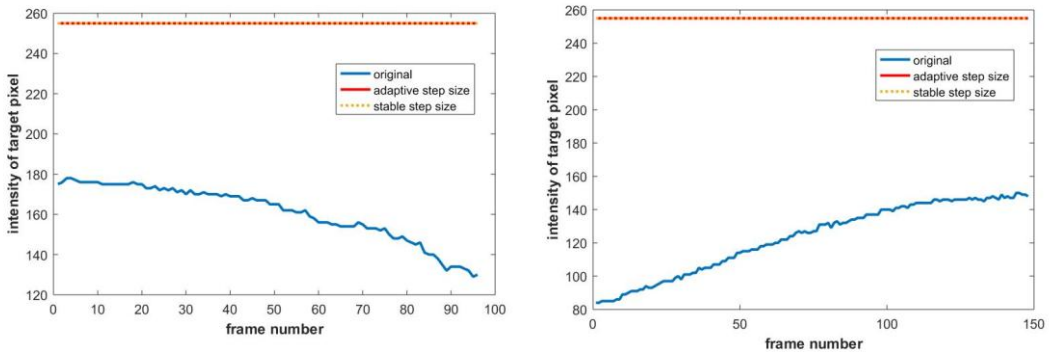

Fig. 4 Comparison between adaptive and fixed step size

[16] proposed an adaptive step size selection strategy. We control the value strategy and calculation method of other variables consistent, use fixed step size 10^{-6} and adaptive step size , for sequences with average SCR = 1.09 and SCR = 1.13, the target enhanced results are shown in Fig.4. 10^{-6} is the reasonable value determined according to the above argument, while the adaptive step size is based on the optimal value in [16]. In each of the two figures in Fig. 4, the lower curve represents the intensity of the target in the original image sequence, and the upper two curves are the intensity curves enhanced by the fixed step and the adaptive step respectively (completely overlapped). It can be seen that under the condition of two step size values, the target can achieve the same optimal enhancing effect.

2.3 Normalization

The background suppression stage produces an estimate of each pixel, the residual image of original image and background estimation image contains the target, the residual clutter, the detector noise area and the isolated noise points. In this case, the normalization is required to adjust the quantization bits of the gray level to specific bits. For the image that has been suppressed (denoted as$I_{back_suppress}$), in which the maximum gray value is $max\ (I_{back\_suppress})$ and the minimum gray value is $min(I_{back\_suppress})$, for each pixel (x, y), normalize the image to a specific gray scale according to the following formula:

$$I_{nor} = (2^n - 1) \times \frac{I_{back\_suppress}(x,y) - min\ (I_{back\_suppress})}{max(I_{back\_suppress}) - min(I_{back\_suppress})} \quad (4)$$

Where, n is the number of quantization bits. In this paper, we take 8, that is, the gray value range is 0 ~ 255, and the normalized image is denoted asI_{nor}, which is the input of the next step.

3. TARGET RE-ENHANCEMENT BASED ON GRAY SCALE DIFFERENCE

TDLMS preprocess can suppress most of the background, at this procedure the target is enhanced for the first time. However, in the residual image, the background clutter (mainly cloud edge), the isolated noise, the detector inherent noise region and the small background of the artificial noise are all included along with the target region. The next operation is mainly for screening out all non-target clutter content. The clutter exists mainly in the following forms: (1) the isolated noise point, the high-brightness point introduced by the complex reasons. It is very similar to the target in single frame. Therefore, it is difficult to screen out in single frame but need to be removed in the multi-frame association phase; (2) the residual background clutter region, which is inevitably generated by the background prediction algorithm, which can be removed by the threshold segmentation of the neighborhood gray-scale difference metric threshold segmentation; (3) detector inherent noise, which shows similar characteristics when presented on image for each frame, different detectors introduce different noise and therefore produce different clutter shapes in the image sequences, which can be removed by means of connected domain processing method. In this section, Re-enhancement algorithm is introduced.

3.1 Neighborhood Gray Scale Difference

In the re-enhancement algorithm presented in this section, the part that gets the segmentation threshold is partially based on mathematical morphology white top-hat operation. Therefore, the concept of white top-hat is first introduced here. Mathematical morphology was first proposed by Serra and Matheron[18] and extended to the field of image processing, and then a number of algorithms based on this improvement and algorithm migration have been proposed[19]. Its essence is the use of a certain size of the structural elements to perform logical operation with each pixel in the image. Assume that a certain pixel of the original image X is$f(x, y)$,

the structural element is B, where a certain element is$B(p,q)$, and several basic morphological transformations are as follows:

(1) Dilation: $f \oplus B = max\,(f(x-p, y-q))$

(2) Erosion: $f \ominus B = min\,(f(x+p, y+q))$

(3) Open: $f \circ B = (f \ominus B) \oplus B$

(4) Close: $f \cdot B = (f \oplus B) \ominus B$

(5) White top-hat: $White\ top\_hat = f(x,y) - f \circ B(x,y)$

(6) Black top-hat: $Black\ top\_hat = f \cdot B(x,y) - f(x,y)$

Dilation operation is mainly used for filling the small area, the erosion operation is to filter out the small bright thorns, open operation is to eliminate small objects, smooth boundary, close operation mainly fills within the area of small holes, connects the adjacent area to smooth the border. The white top-hat transformation, based on the open operation, highlights the target points, while the black top-hat transformation bases on the close operation and predicts the background area.

After the above analysis, we can see that for the preprocessed images after background suppression, the aim at this period is to filter out the residual background clutter and other clutter interference introduced by the algorithm. Therefore it's naturally to take white top-hat operator into consideration. But directly using the white top-hat operator to highlight the bright area does not distinguish between the target and the clutter, but to enhance all the adjacent areas of high contrast area. Therefore it is necessary to find a threshold for segmenting the target and clutter. Draw on the idea of [19], we get the following processing.

As for morphological open operation, the image is first eroded and then dilated. That is, for each pixel, minimum of neighborhood is taken to form an erosion image, then for each pixel in this erosion image, maximum of neighborhood is taken. Respectively, target pixel and clutter pixel are $(x_T, y_T)$and(x_c, y_c), since the target has been significantly enhanced after the preprocessing part in first step, its intensity must be greater than the other pixels of its neighborhood, then its gray value is much greater than its open operation value. Therefore, the white top-hat value of (x_T, y_T) obeys the relation:

$$white\ top\_hat(I_{nor}(x_T, y_T)) = I_{nor}(x_T, y_T) - I_{nor} \circ B(x_T, y_T) > 0 \quad (5)$$

The experimental results after the background suppression phase show that most of the clutter is still a block or striped area, not a point of isolation, and the brightness is much smaller than the enhanced target, so for most of the clutter region, a certain pixel(x_c, y_c), respectively, obeys the relation:

$$white\ top\_hat(I_{nor}(x_c, y_c)) = I_{nor}(x_c, y_c) - I_{nor} \circ B(x_c, y_c) < 0 \quad (6)$$

$$or$$

$$I_{nor}(x_c, y_c) - I_{nor} \circ B(x_c, y_c) \to NaN \ (7)$$

It means that the white top-hat value of a clutter pixel is tend to be a very small positive value or even a negative value.

Based on the above, a proper threshold is needed to distinguish between the target and the clutter. Thus, a neighborhood gray-scale difference metric is introduced here to filter out clutter points that interfere with the target detection. In order to ensure the fastest calculation speed, for each pixel(x, y) of the image I_{nor}, a sliding window is set to scan the image from left to right and top to bottom, and the maximum gray value of the

neighborhood covered by current window is denoted by max_value, and the minimum gray value is min_value, the center value, which is describes as gray-scale difference(GSD) value, is denoted as:

$$GSD(x,y) = max\_value - min\_value \quad (8)$$

Simply, we take $GSD(x,y)$ as the neighborhood gray-scale difference of the current pixel. After all the pixels in the image is scanned, it forms the difference measure image, denoted as $X_{Estimate}$. The adaptive threshold formed by mean and standard deviation of $X_{Estimate}$ is as follows:

$$T = mean(X_{Estimate}) + \alpha \cdot \sigma \quad (9)$$

In the above equation, σ is the standard deviation of $X_{Estimate}$, α is an adjustment parameter. The value of α will be described in detail in Section 3.2. It is known from the above equation that the target pixel has little effect on the whole of $X_{Estimate}$ because the target size is very small, but the brightness of the enhanced target is greater than that of most of the clutter brightness. Therefore, for the target pixel(x_T, y_T), it is more likely that its white top-hat value is greater than T, while for a clutter pixel (x_c, y_c), even if its gray value is greater than T, its white top-hat value is small, therefore we can use this kind of difference to distinguish between target and clutter pixel.

After the target re-enhancement process, the clutter suppression image based on the neighborhood gray-scale difference metric and morphological top-hat is formed, which is denoted as $I_{clutter\_suppress}$, for each pixel (x,y) of $I_{clutter\_suppress}$, the corresponding value obeys the following formula:

$$I_{clutter\_suppress}(x,y) = max(white\ top\_hat(I_{nor}(x,y)), T) - T \quad (10)$$

Where,

$$White\ top\_hat(I_{nor}(x,y)) = I_{nor}(x,y) - I_{nor} \circ B(x,y) \quad (11)$$

$$I_{nor} \circ B(x,y) = \max_{(p,q)} \{ \min_{(p,q)} [I_{nor}(x-p, y-q) + B(p,q)] \} \quad (12)$$

$B(p,q)$ is an element of structural element.

From above, if a certain pixel, denoted as(x,y), is a target pixel, then:

$$white\ top\_hat(x,y) > T$$

$$I_{clutter\_suppress}(x,y) = white\ top\_hat(x,y) - \mathrm{T}$$

If it is a clutter pixel, then it is of great possibility that:

$$white\ top\_hat(x,y) < T$$

$$I_{clutter\_suppress}(x,y) = 0$$

Therefore, after the above treatment, a large amount of the residual clutter will be filtered out.

3.2 Selection of α

In general, α is the value of the target intensity, if the target brightness is smaller, the value of α is smaller, otherwise, the value is larger. According to the essence of GSD, if the target intensity is large, the algorithm focuses on reducing the false alarm rate, so a larger threshold T should be set, then the value of α can be larger; if the target intensity is smaller, the algorithm focuses on improving the target detection probability, it can set a smaller threshold T, then the value of α may be smaller. The setting of the threshold T conforms to the general setting rule of the adaptive threshold based on the image mean, variance and signal-to-noise ratio, and α is the signal to noise ratio of $X_{Estimate}$. It is calculated as follows:

$$\alpha = \frac{median(M_T) - mean(M_B)}{\sigma_{M_B}} (13)$$

In the above formula, M_T refers to the target area, $median(M_T)$ is the median of the target area intensity, M_B refers to the background area, and $mean(M_B)$ is the average of the background area intensity. σ_{M_B} is the standard deviation of the background area.

4. INFRARED POINT TARGET DETECTION

4.1 Connected Domain Segmentation

Section 3 begins with the description of the clutter category, Section 3.1 describes the algorithm for residual background clutter removal. This part focuses on system inherent noise. The area of this kind of noise, which is blind or flash element when reflected in the image, is largely due to the inconsistency of the response of the space-borne detector. Unlike isolated noise points, this part of the clutter is jammed into lumps and is about tens of pixels, which is larger than the target size. Therefore, it is possible to filter the oversized clutter domain by constructing connected domains. For re-enhanced image $I_{clutter\_suppress}$, connected domain segmentation operation is as follows:

$$I_{clutter_{suppress}}(S_i \le T_{low} \parallel S_i \ge T_{high}) = 0, S_i \subseteq \Phi \quad (14)$$

Where, $i = 0,1,\dots,length(\Phi)$, Φ is the set of all isolated areas in $I_{clutter\_suppress}$. T_{high} and T_{high} are the low and high boundaries, respectively. They represent the smallest and largest detector noise area, respectively, and can be valued according to practical application environment. It is worth mentioning that the probability of the detector noise area being smaller than the target size is extremely small, so in most cases the above equation can be simplified as:

$$I_{clutter_{suppress}}(S_i \ge T_{high}) = 0,, S_i \subseteq \Phi (15)$$

Before connected domain processing, a mathematical morphological dilation operation is usually implemented, which is designed to connect the cracked flash element area. Because the target presents as an isolated point state, the dilation operation may not have an impact on target shapes, centers and so on. Take a certain frame as an example, the connected domain segmentation results are shown in Figure 5. Several large areas of clutter have been marked with red rectangles, indicating that the distribution of clutter points in the connected domain can be effectively removed.

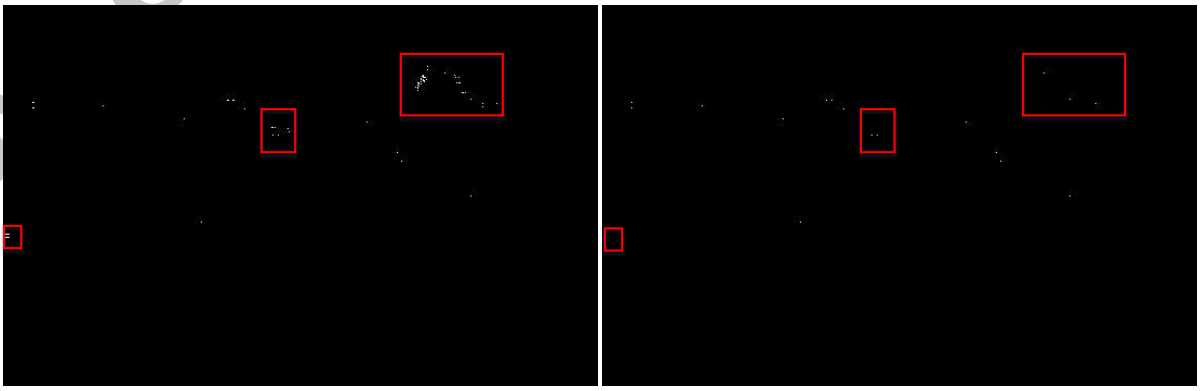

(a) (b)

Fig. 5 Comparison before and after connected domain segmentation. (a) Before the extraction of detector inherent clutter area (b) After the extraction using connected domain segmentation.

4.2 Multi-frame trajectory association

This part aims at filtering out isolated noise, and extract target track. Since the real space-based target motion has regularity (this article assumes that the target moves at a constant speed), the trajectory is associated in adjacent frames, however, the correlation between the noise pixels in each frame is approximately zero, then these two can be distinguished accordingly. For targets with a speed of no more than 1 pixel/s, candidate target's 8- neighborhood is searched in each frame, based on the continuity of the target motion, that is, based on Figure 6, ignoring the target cross-pixel effect, if there is no case of missing or dropped frames in the detection of each frame, then the 8 neighborhood of the target pixel is supposed to contain a potential target pixel in next frame, that is, as Figure 6 shows, as for the current target pixel P, the position of the target in next frame is one of N1-N8.

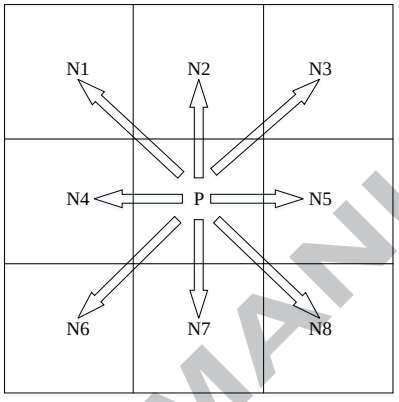

Fig. 6 3×3 sized neighborhood (8-neighborhood) of the current pixel. The arrows are possible directions of target movement.

Here, we limit the target velocity less than 1 pixel/frame. In fact, there is no clear limitation on the speed of the target. It is because the algorithm model TDLMS_GSD proposed in this paper can detect targets at variable velocities, not only able to detect the target with velocity less than 1 pixel/frame in x or y direction. The reasons that this article limits the targets have rate≤1pixel/frame in x direction and y direction are as following:

a) Explore algorithmic performance in more extreme environments. In fact, the detection of slow targets is even more challenging than fast targets for space target detection algorithms. Because the target is accompanied by movement of the satellite platform movement, the background of the movement, etc., which brings more difficulties for detection.

b) Simplify the process of trajectory association. The core part of the algorithm proposed in this paper is mainly focused on the background suppression and target enhancement spatial processing, rather than focusing on the trajectory extraction or time-domain processing. The reasonable algorithmic model of space-time target tracking is the focus of the next part of this dissertation.

Signal-to-clutter ratio of the image sequence experimented in this paper is very low (SCR≈1). In such situation, it is inevitably that there are missed target for a small number of individual image frames. Therefore, in the actual process, we extend the search range to two frames, that is, if the current candidate of the 8-neighborhood of the current potential target pixel does not contain the candidate target point in the next frame, then next frame is continuously searched, with the searching window of 5×5 sized neighborhood. If there is a candidate target point, the current scanned pixel is judged as a target point, and if there is not, it is considered as an isolated noise pixel. If the length of the resulting trajectory is greater than the preset threshold (one frame is allowed to be

lost), then the trajectory is saved, otherwise it is removed. In this way, the target trajectory is extracted by the multi-frame association, and the noise pixels independently distributed per frame are eliminated.

According to Section 2, Section 3 and Section 4, we get the overall flowchart of the proposed processing model, as shown in Figure 7.

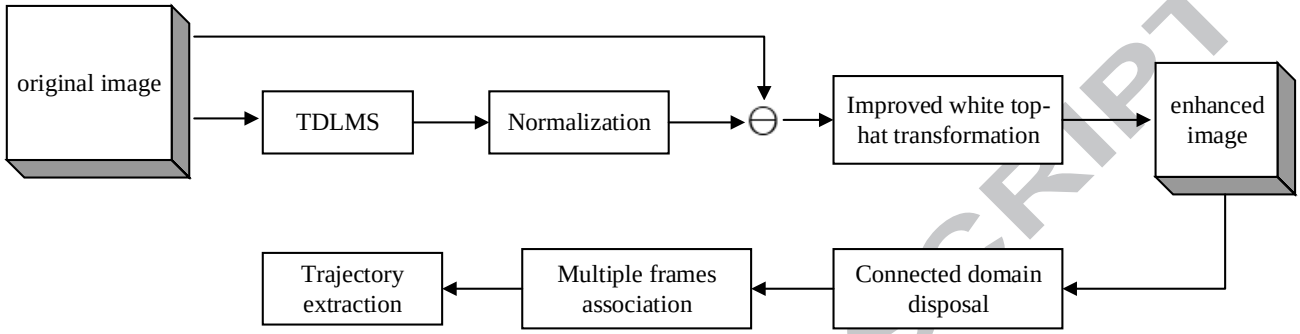

Fig.7 Flowchart of the proposed whole algorithm model

4.3 Computational complexity

In the preprocessing stage, the main complexity of the algorithm is the overhead of running TDLMS filter, which includes the complexity of obtaining the pixel estimation value and the weight update, that is, the costs of equation (1) and (2). For each R × R neighborhood of each pixel in the M × N image, the calculation of (1) is carried once, therefore the overhead is $O(R^2 \cdot M \times N)$; for (2), each pixel is calculated, so the complexity is $O(M \times N)$. In the target re-enhancement stage based on neighborhood gray scale difference, the main complexity of the algorithm lies in the calculation of GSD image, the image white top-hat operation and the re-enhancement of the image. For preprocessing image I_{nor}, we need to get the maximum and minimum values of each pixel in $\mathrm{R} \times \mathrm{R}$ neighborhood (R^2 pixels in total), and assign once. Therefore, the total complexity of the process of taking the maximum and minimum values is $O(2 \cdot (R^2 - 1) \cdot M \times N)$. The complexity of the assignment process is $O(M \times N)$. The white top-hat operation needs to erode the image I_{nor} before performing dilation operation (that is, open operation), and then subtract the result of the open operation from the original image I_{nor}. During the erosion process, each pixel takes the maximum value of $\mathrm{R} \times \mathrm{R}$ neighborhood, the complexity of the whole image ($\mathrm{M} \times \mathrm{N}$ pixels) is $O(R^2 - 1)$, there is another assignment process, the complexity is O(1), so the complexity of the erosion operation for the whole image ($\mathrm{M} \times \mathrm{N}$ pixels) is $O(R^2 \cdot M \times N)$; similarly, the dilation process is taking the minimum value in the $\mathrm{R} \times \mathrm{R}$ neighborhood of each pixel, the complexity is equal to that of the erosion operation, that is $O(R^2 \cdot M \times N)$; the white top-hat also includes a subtraction operation with a complexity of $O(M \times N)$. According to equation (10), each pixel contains a comparison and an assignment process for acquisition of $I_{clutter\_suppress}$, so the total complexity is $O(M \times N)$.

Therefore, the total computational complexity of the proposed method is the complexity sum of preprocessing and target re-enhancing, that is $O((5R^2 + 1) \cdot M \times N)$. Constant number can be neglected and the complexity is simplified as $O(R^2 MN)$(The neighborhood window is much smaller than the width of the image,$\mathrm{R} \ll \mathrm{M}$ and $\mathrm{R} \ll \mathrm{N}$).

We summarize the computational complexity of several target-enhancing algorithms listed in the Introduction section, and summarize the results into the following Tab.1. The algorithm listed in Tab.1 are as comparison algorithms, details of the implementation and the results of the experiment will be given in the experiment

results part. From Tab.1, TDLMS_GSD can achieve the same computational efficiency as the other state-of-art algorithms, with a lower degree of complexity than the max-median algorithm.

Tab.1 Comparison of computational complexity for TDLMS_GSD and several other algorithms

Algorithms	Max-mean	Max-median	TDLMS	TDLMS_Cao	TDLMS_edge	TDLMS_neighbor	TDLMS_GSD
Complexity	$O(R^2MN)$	$O(R^2\log(R^2)MN)$	$O(R^2MN)$	$O(R^2MN)$	$O(R^2MN)$	$O(R^2MN)$	$O(R^2MN)$

5. EXPERIMENTAL RESULTS

5.1 Selection of Parameters and Performance Index

In this paper, 5 different image series with image size 256×320 are used as the background image, among them, three sequences are simulation image sequences (infrared sequences of background LEO satellites) with superimposed target, recorded as S1, S2 and S3, respectively; the other two sequences are real target image sequences taken by space-borne low-orbit infrared cameras with a detection range of 1000km, denoted as R1 and R2. The simulation targets in S1, S2 and S3 are superimposed according to the real space-based environment. Simulation objectives take full account of the atmospheric transmittance, optical efficiency, optical system F number, platform jitter and other factors. The parameters are set as shown in Table 2. The simulation target is generated according to the point spread function.

Tab. 2 Parameter setting and value of the simulation

Parameter name	Value
Detection distance	≤1000 (km)
Atmospheric transmittance	0.8
Optical system F number	3
Optical system diameter	1 (m)
Optical efficiency	0.2
Pixel size	1.667×10^{-5} (m)
The number of sinusoidal signals in platform jitter	10
Amplitude of sinusoidal signal in platform jitter	[2,3,2,3,2,4,2,3,3,2]
The frequency of sinusoidal signal in platform jitter	[50,60,70,80,90,100,110,120,130,140]
Energy concentration variance	44.2
Target radiation intensity (W/SR)	1×10^{7}

An important factor in the effectiveness of simulation images is the size of the simulation target. According to the parameters in Table 2, we can estimate the range of targets covered by a certain size on the image plane, that is, the number of pixels the target occupies on the image. In fact, the size of the target on the image plane is related to the resolution, sensitivity and other parameters of the detection system. In order to simplify the problem, the indirect influencing factors are not considered. Assuming that the real target size L of the detection is 20m, the estimation formula for the target size N_{target} on the image plane is obtained according to the system parameters:

$$N_{target} = \frac{L\cdot F\cdot d}{D\cdot k} \quad (16)$$

In the above formula, F is the optical system F number, d is the optical system aperture, D is the detection distance, k is the pixel size. Assuming that the detection distance at this time is the maximum, then by bringing

in the relevant value in Table.2 into the above equation, N_{target} value can obtained. The calculation process is as follows:

$$N_{target} = \frac{20 \times 3 \times 1}{1000 \times 10^3 \times 1.667 \times 10^{-5}} \approx 3$$

Therefore, we set the target size as 3 × 3 in this paper.

Before point target detection is performed, background suppression and target enhancement is critical, while measuring target enhancement performance is mainly based on single-frame signal-to-clutter gain. The calculation of the signal to clutter ratio (SCR) is based on the calculation of the complexity of the image:

$$SCR = \frac{T_{average} - \mu}{\sigma} \quad (17)$$

Where, $T_{average}$ is the average brightness of target, μ is the average brightness of the background, σ is the standard deviation of the image, the signal-to-clutter gain equation is defined as:

$$SCR_{gain} = 20 \log_{10} \frac{SCR_{out}}{SCR_{in}} \quad (18)$$

SCR_{out} is the SCR after GSD algorithm while SCR_{in} is the SCR of the original image. SCR_{gain} uses dB as unit. Correspondingly, the performance evaluation for background suppression is mainly based on background suppression factor (BSF)[20], and the formula is:

$$BSF = \frac{\sigma_{in}}{\sigma_{out}} \quad (19)$$

σ_{in} is the standard deviation of the original image, $\sigma_{out}$is the standard deviation of the proposed image after background suppression GSD algorithm but before connected domain processing.

In the experiment, there are several windows that needed to be set up in the processing of the algorithm. In this experiment, the window size is set to 3 × 3 (including the structural element B of the morphological operation), except for local SCR calculation window, which is set to 13×13 with radius 6.

5.2 Experimental Results

By using the detection model TDLMS_GSD presented in this paper, five sequences are processed and the results of several random frames of five sequences are summarized respectively, as shown in the following Fig.8.

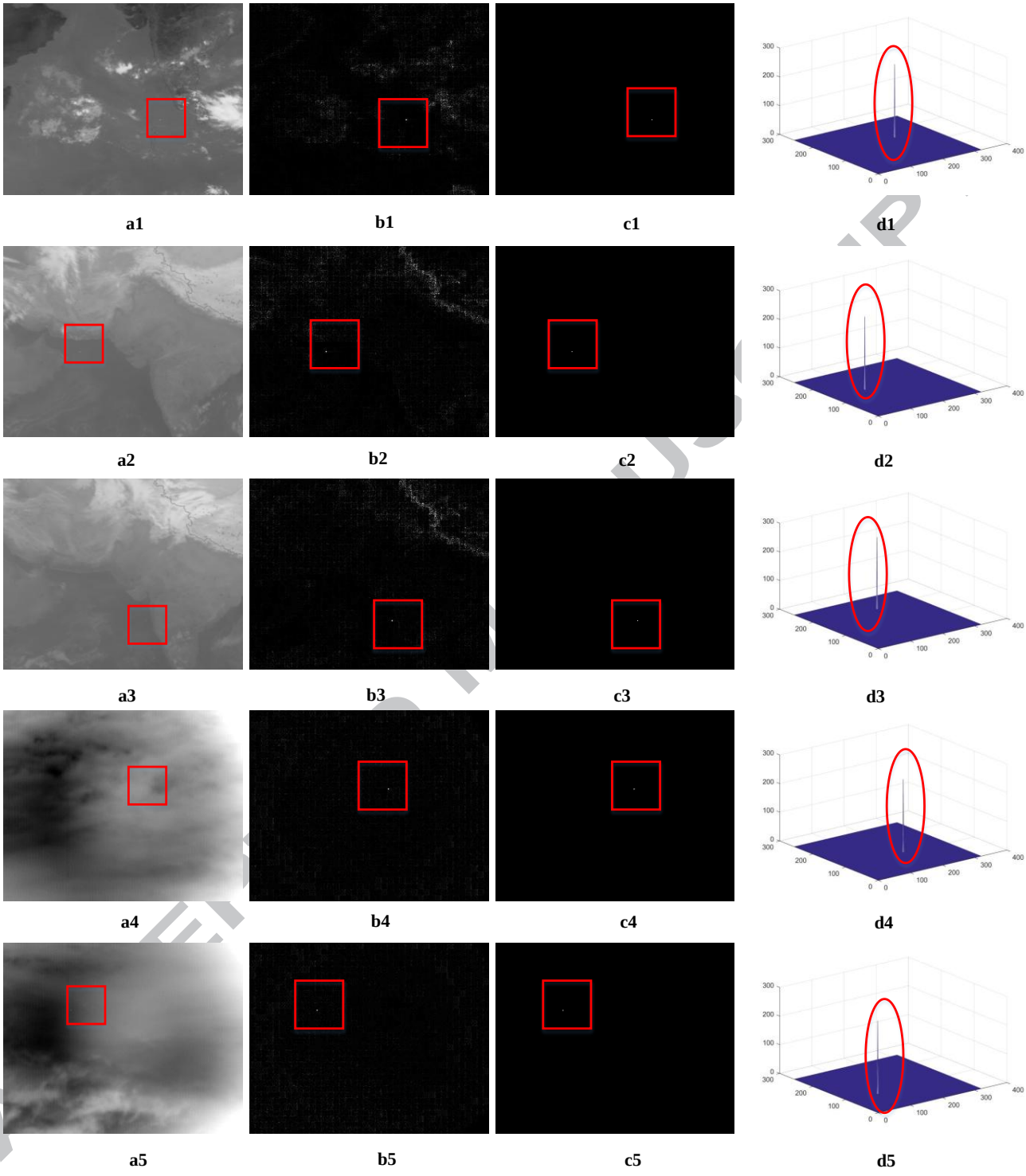

Fig.8 Results of different image sequences/backgrounds.a1-a5 are the original frames; b1-b5 are results after TDLMS; c1-c5 are re-enhanced results after GSD based algorithm; d1-d5 represent density distribution diagrams of detection. The box part is marked with the current target position, the ellipse marks the location of the target。

In the above figure, b1-b5 are the results of preprocessing by TDLMS, c1-c5 are the results of the re-enhancement by using GSD-based enhancement algorithm, and d1-d5 represent the final detection results. The experimental results show that the proposed algorithm can predict the background of image sequences with different background features. c1-c5 are the results of image enhancement based on GSD. The essence of this

algorithm is to filter out the background again. We can see that in b1-b5, part of the existing edge clutter in c1-c5 can be well filtered out. d1-d5 are the detection results, the circled part represents the target intensity, which denoted that the target can be effectively detected.

Fig.9 shows the results of several algorithms, and the results are plotted as density figures. Each column in Fig.9 represents a detection result of an image sequence. Starting from the second row, each row represents an algorithm, max-mean, max-median, original TDLMS, Cao'TDLMS, edge directional TDLMS, improved TDLMS based on neighborhood information, and TDLMS_GSD proposed in this paper, respectively. The description of several improved TDLMS methods is as follows.

(1) Cao's TDLMS ([15])

Mainly to solve the two problems existing in the original TDLMS: 1. One window cannot fully consider the neighborhood information and thus causes center pixel estimation deviation. 2. The step size cannot be adjusted adaptively. For both of these problems, the algorithm proposes improvements. For Problem 1, this method expands the window by replacing one of the previous windows with five adjacent windows, estimating the center pixel by synthesizing gray information of five same-sized windows. For problem 2, when the center window covers the target pixel, the four surrounding windows have a more similar grayscale distribution, and the step size μ should be reduced. When the center window covers the background edge pixels, the surrounding four windows have a greater difference of grayscale distribution, and the step size μ should be increased. Therefore, the problem of adaptive step size is transformed into the problem of measuring the similarity of the four windows' grayscale, which can be solved by "scattering criteria" in pattern recognition theory.

(2) edge directional TDLMS ([16])

Mainly to solve the background edge problem. The method suggests that when a target pixel at the edge of cloud is as the center of a window, setting one window cannot effectively distinguish it. The solution is to extend the original one window to nine windows of the same size, calculate the difference between the left diagonal, the right diagonal, the horizontal diagonal and the vertical diagonal respectively(the central window is not counted). The two windows with the smallest difference are as the main basis for updating the weights and updating the predicted value. Meanwhile, the adaptive selection of the step size μ is also discussed, by setting a maximum step size μ_{max} and the minimum step size μ_{min}, taking the logarithm of the mean square error of the central prediction value obtained from the above eight neighborhood windows as function coefficients, fine-tuning μ. For the calculation of adaptive step size μ, the formula is as follows:

$$\mu(m,n) = \frac{\mu_{max}-\mu_{min}}{1+e^{-log\,(\sigma^2{}_{g(m,n)})}} \quad (20)$$

(m,n) is the current pixel, and $g(m,n)$ is a vector composed of the central prediction values of 8 neighborhood windows.

(3) TDLMS based on neighborhood information ([17])

An improved algorithm for edge directional TDLMS. It replaces the original edge-based output with neighborhood-based output. Similar to the edge-directional TDLMS, nine prediction windows are provided in conjunction with the central window. The principle based on the neighborhood information is that if the prediction of the central window is greater than the surrounding eight ones, it is possible that the central window covers the target area , in order to ignore the small target, the predicted value should be as small as possible and the gray difference as large as possible, then the filter output is the average of the two minimum in eight

predicted values; if the above relationship is not satisfied, then it is possible that the current window center is in the background area, then the predicted value should be kept as close as possible to the true value. Therefore, the average of the two values that have the smallest difference with the center window predicted value is taken as the filter output value.

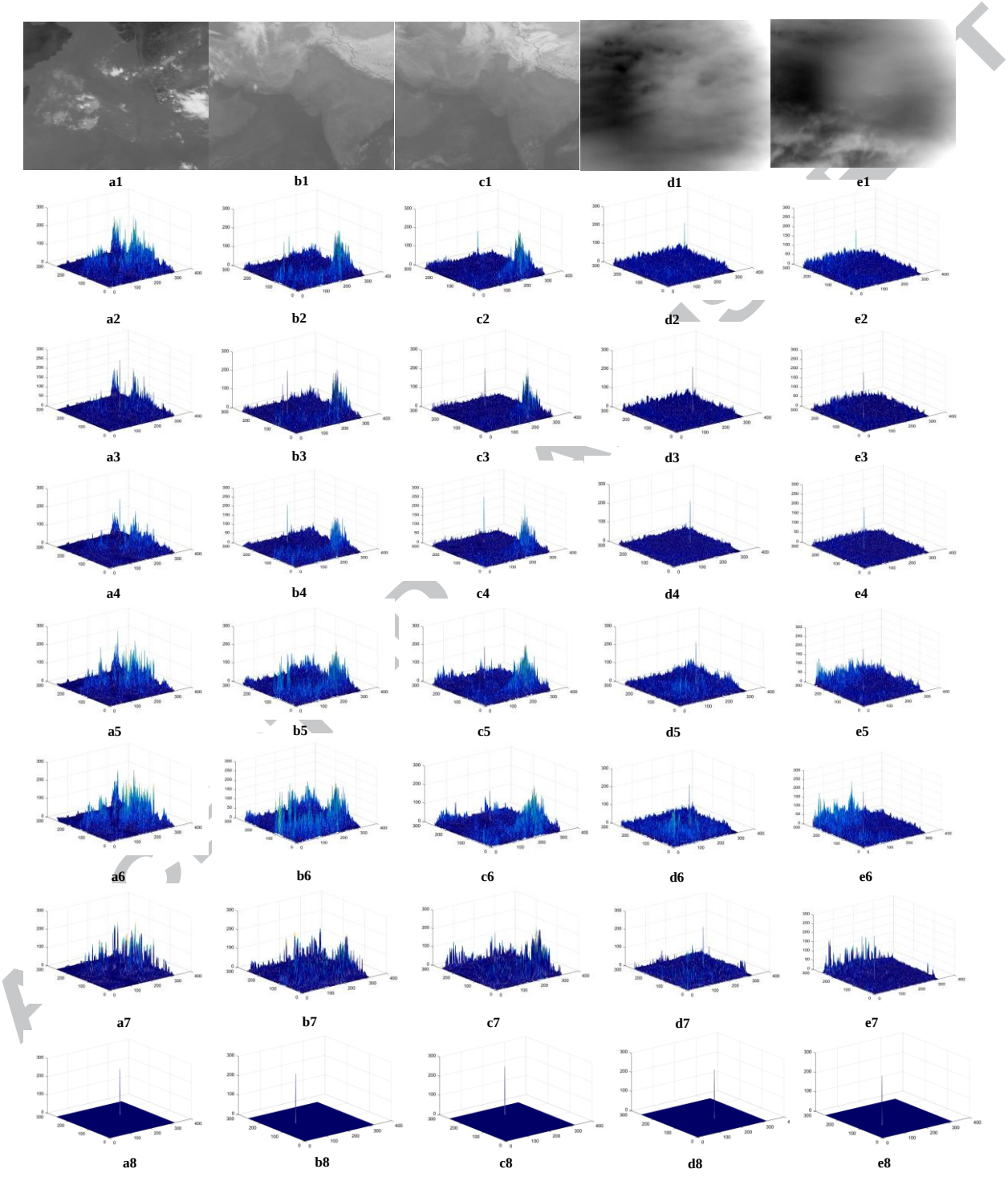

Fig. 9 Results of different background suppression algorithms. a1-e1 are the original frames of different sequences. From the second to the last line, the application of the algorithm are: max_mean, max_median, traditional TDLMS, Cao's TDLMS, edge directional TDLMS, TDLMS based on neighborhood information, and TDLMS_GSD proposed in this paper.

Density figure represents the intensity of each pixel. Therefore, compared with several other state-out-art enhancement algorithms, the algorithm model proposed in this paper can reduce the false alarm rate to a greater extent. In addition to the classical TDLMS algorithm and the enhancement algorithm proposed in this paper, the results of the algorithm, including max_mean, max_median, TDLMS proposed by Cao et al., edge-oriented TDLMS and TDLMS based on neighborhood information, are not very good, the target is completely mixed in the residual clutter. This is due to the extreme complex background and cloud background ups and downs in this context, there is almost no smooth distribution of the situation, so the edge-based or neighborhood-based filter improvement make the central pixel prediction value inaccurate.

Table 3 is a quantitative description of the comparison algorithms. According to the statistics of Table 3, for several processing algorithms, the SCR_gain and BSF are quantitatively compared. For same situation, the proposed algorithm (TDLMS_GSD) has the best performance in background suppression and target enhancement.

Tab. 3 Summary of different algorithm processing results with different SCR sequences

Image Sequence	Original SCR	Algorithm	Processed SCR	SCR_gain	BSF
S1	1.74	max-mean	14.51	18.28	1.24
		max-median	24.31	21.80	2.13
		TDLMS	30.03	24.67	2.12
		TDLMS_Cao	12.19	16.80	1.39
		TDLMS_edge	9.17	14.40	1.20
		TDLMS_neighbor	10.43	15.36	1.59
		TDLMS_GSD	277.13	44.04	19.32
S2	1.09	max-mean	10.86	19.72	1.94
		max-median	14.94	21.29	2.71
		TDLMS	20.34	25.27	2.42
		TDLMS_Cao	10.52	19.57	1.88
		TDLMS_edge	8.17	17.37	1.74
		TDLMS_neighbor	9.28	18.47	2.24
		TDLMS_GSD	90.96	38.22	10.31
S3	1.02	max-mean	11.49	20.69	2.42
		max-median	15.70	22.42	3.29
		TDLMS	21.28	26.16	2.84
		TDLMS_Cao	12.26	21.45	2.12
		TDLMS_edge	9.62	19.33	1.89
		TDLMS_neighbor	12.46	21.59	2.23
		TDLMS_GSD	89.49	38.59	11.34
R1	0.55	max-mean	27.23	33.65	5.94
		max-median	34.46	34.86	7.51
		TDLMS	50.01	38.99	10.81
		TDLMS_Cao	26.21	33.46	5.74
		TDLMS_edge	21.62	31.79	4.79
		TDLMS_neighbor	35.77	36.16	7.74
		TDLMS_GSD	262.58	53.44	55.62

		max-mean	25.99	32.87	5.47
		max-median	33.83	33.98	7.18
		TDLMS	49.39	38.65	10.29
R2	0.57	TDLMS_Cao	23.07	32.04	4.88
		TDLMS_edge	17.63	29.71	3.77
		TDLMS_neighbor	29.06	34.05	6.07
		TDLMS_GSD	262.71	53.12	53.68

SCR_gain is generated according to the formula (18). One SCR gain is obtained for each frame, and the value of SCR_gain in the table is the average of all the SCR_gains in the sequence. "Processed SCR" represents the average SCR level after the algorithm is processed. BSF is calculated according to equation (19), larger BSF value represents a better background suppression effect. The experimental results show that TDLMS_GSD can effectively enhance and detect both simulated targets and real targets with various background types, and is superior to other algorithms in terms of significant metrics.

For the five image sequences, the SCR enhancement of TDLMS_GSD is calculated respectively. Fig.10 shows the validity of the algorithm more intuitively, in which the global and local SCR comparison are presented.

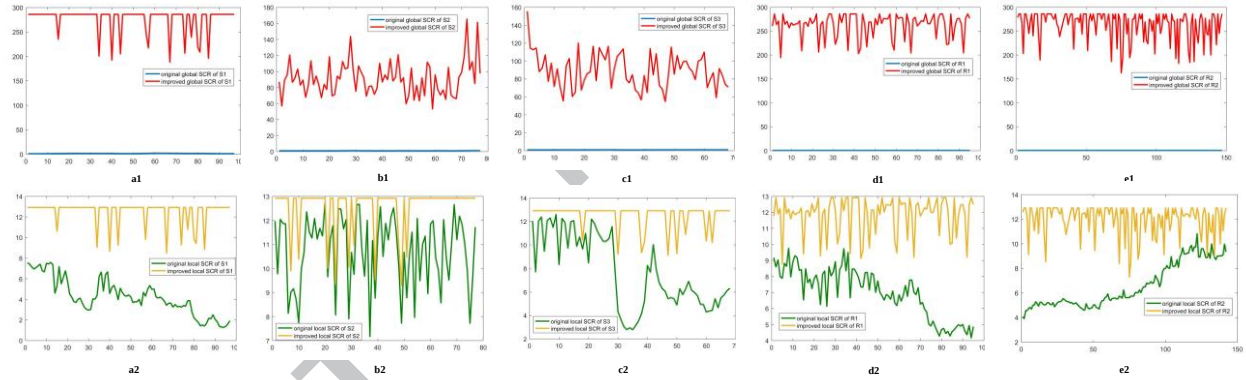

Fig.10 SCR comparison before and after proposed algorithm. a1-e1 are global SCR comparison for 5 sequences; a2-e2 are SCR comparison for 5 sequences in 13×13 sized neighborhood.

In Fig.10, a1-e1 represents the global SCR contrast. The implementation of the algorithm improves the SCR of each frame image in the sequence. The same conclusion also applies to the case of local SCR enhancement represented by a2-e2. It is worth mentioning that the enhanced SCR is difficult to reach a steady state, which is caused by the inherent characteristics of low SCRs and complex background.

Through the process of connected domain segmentation and trajectory association, the screening process of moving objects in five background sequences is completed, results are summarized in Fig.11. Isolated noise has been mostly removed, which proves the effectiveness of the overall algorithm processing model. It can be seen from the final experimental results that the proposed algorithm model can effectively detect targets and extract tracks in image sequences with different backgrounds.

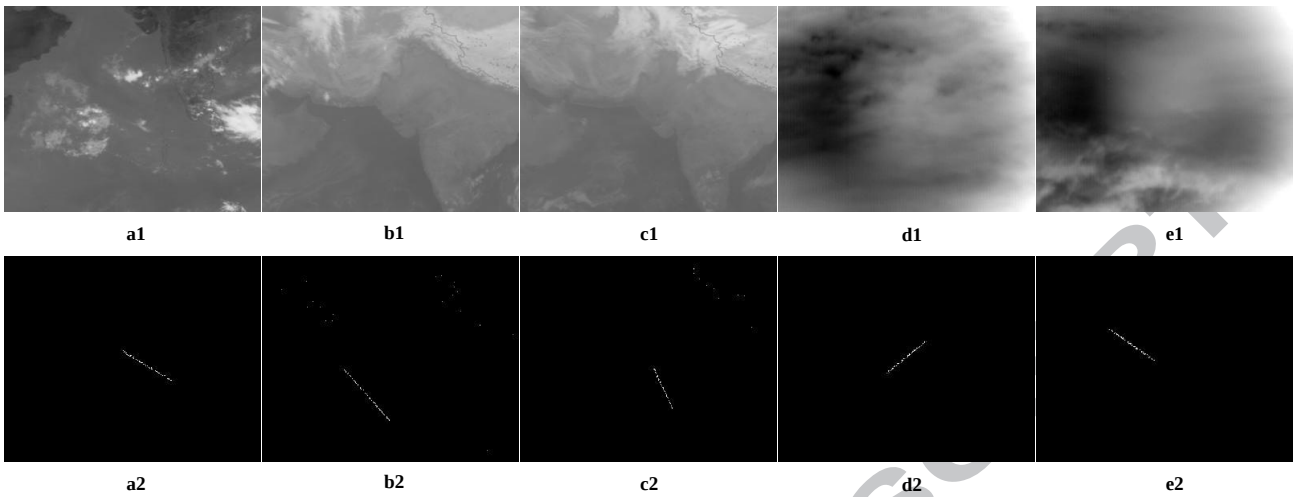

Fig. 11 Multi-frame association results for different sequences

6. CONCLUSION

A new background suppression, detection and trajectory correlation model is proposed in this paper, which focuses on the detection of moving points in the case of low SCR in space-based environment. It first removes the internal background clutter based on the two-dimensional least mean square filter, and then filters the residual background clutter byre-enhancement algorithm based on GSD. Through the connected domain segmentation, the flash area caused by detector response non-uniformity are filtered out, and finally through the multi-frame association the isolated noise is eliminated and target tracks can be extracted. The experiment results show that the detection effect is good in the case of average SCR ≈ 1 or SCR <1. Compared with other state-of-art algorithms, the background suppression and target enhancement performance proposed in this paper are the best. The next step in this paper will focus on the target trajectories of irregular trajectories and the adaptive detection of multi-objective and different-size targets to accommodate more complex space-based environments.

Reference

[1] Chen Y.W, Xin Y.H. An Efficient Infrared Small Target Detection Method Based on Visual Contrast Mechanism[J]. IEEE geoscience and remote sensing letters. 2016, 7, 13(7):962-966.

[2] Wan M, Gu G, Qian W, et al. Robust infrared small target detection via non-negativity constraint-based sparse representation[J]. Applied Optics, 2016, 55(27):7604.

[3] Han J, Ma Y, Huang J, et al. An Infrared Small Target Detecting Algorithm Based on Human Visual System[J]. IEEE Geoscience & Remote Sensing Letters, 2016, 13(3):452-456.

[4] Hadhoud.M.Mohiy, Thomas.W.David. The two-dimensional adaptive LMS(TDLMS) algorithm[J]. *IEEE transctions on circuits and systems*. 1988,5, 35(5):485-494.

[5] Zeng.M, Li.J.X, Peng.Z. The design of top-hat morphological filter and application to infrared target detection[J]. *Infrared Physics&Techonology*. 2005,48:67-76.

[6] Bai.X.Z, Zhou.F.G, Xue.B.D. Infrared dim small target enhancement using toggle contrast operator[J]. *Infrared Physics&Technology*. 2012, 55:177-182.

[7] Deshpande SD, Er MH, Ronda V, Chan Ph. Max-mean and max-median filters for detection of small-targets. Proceedings of SPIE 1999,3809:74–83.

[8] Buades.A, Coll.B, Morel.J.M. A non-local algorithm for image denoising[C]. *2005 IEEE computer society conference on computer vision and pattern recognition*. 2005,2:60-65.

[9] Buades.A, Coll.B, Morel.J.M. Nonlocal image and movie denoising[J]. *International journal of computer vision*. 2008,2.76(2):123-139.

[10] Buades.A, Coll.B, Morel.J.M. A review of image denoising algorithms, with a new one[J]. *SIAM journal on multiscale modeling and simulation*.2005,1. 4(2):490-530.

[11] Genin.L, Champagnat.F, Besnerais.G.L, Coret.L. Point target detection using a NL-means type filter[C]. *2011 18th IEEE international conference on image processing*. 2011:3533-3536.

[12] Deng.H, Wei.Y.H, Tong.M.W. Background suppression of small target image based on fast local reverse entropy operator[J]. IET Computer Vision.2013,7(5),405-413.

[13] Huang.K, Mao.K. Detectability of infrared small targets[J]. Infrared Physics & Technology. 2010,53(3),208-217.

[14] Zhao.F, Zhang.Z.Y, Lu.H.Z. Dim point target detection based on novel complex background suppression[C]. *2012 International conference on computer vision in remote sensing*. 2012,45-51.

[15] Cao.Y, Liu.R.M, Ynag.J. Small target detection using two-dimensional least mean square(TDLMS) filter based on neighborhood analysis[J]. *Infrared milli waves.* 2008, 29:188-200.

[16] Bae T.W, Zhang F, Kweon I.S. Edge directional 2D LMS filter for infrared small target detection[J]. Infrared Physics & Technology. 2012, 55:137-145.

[17] Wan L.L, Wang M. Infrared small target detection using TDLMS filter based on neighborhood information. Journal of Huazhong University of Science and Technology (Natural Science Edition). 2015, 10, 43(I):178-181.

[18] Serra.J, Image analysis and mathematical morphology. New York, USA: Academic Press; 1982.

[19] Bai X.Z, Zhou F.G. Infrared small target enhancement and detection based on modified top-hat transformations [J]. *Computers and electrical engineering*. 2010, 36:1193-1201.

[20] Hilliard C.I., Selection of a clutter rejection algorithm for real-time target detection from an airborne platform, Proc. SPIE 4048 (2000) 74–84.